https://doi.org/10.5194/mr-2020-15
Preprint. Discussion started: 23 June 2020

Open Access MAGNETIC RESONANCE Discussions

Orthogonally spin-labeled rulers help to identify crosstalk signals and improve DEER signal fidelity

Markus Teucher[1], Mian Qi[2], Ninive Cati[2], Henrik Hintz[2], Adelheid Godt[2], and Enrica Bordignon[1]

[1]Faculty of Chemistry and Biochemistry, Ruhr University Bochum, Universitätsstraße 150, 44801 Bochum, Germany
[2]Faculty of Chemistry and Center for Molecular Materials (CM_2), Bielefeld University, Universitätsstraße 25, 33615 Bielefeld, Germany

Correspondence: Enrica Bordignon (enrica.bordignon@rub.de)

Abstract. DEER spectroscopy applied to orthogonally spin-labeled proteins is a versatile technique which allows simplifying the assignment of distances in complex spin systems and thereby increasing the information content that can be obtained per sample. In fact, orthogonal spin labels can be independently addressed in DEER experiments due to spectroscopically non-overlapping central transitions, distinct relaxation times and/or transition moments. Here we focus on molecular rulers orthogonally labeled with nitroxide (NO) and gadolinium (Gd) spins, which give access to three distinct DEER 'channels', probing NO-NO, NO-Gd and Gd-Gd distances. It has been previously suggested that crosstalk signals between individual DEER channels might occur, for example, between NO and Gd due to their inevitable spectral overlap. However, a systematic study to address these issues has not yet been carried out. Here, we perform a thorough three-channel DEER analysis on mixtures of NO-NO, NO-Gd and Gd-Gd molecular rulers characterized by distinct, non-overlapping distance distributions to study under which conditions crosstalk signals occur and how they can be identified or suppressed to improve signal fidelity. This study will help to improve the assignment of the correct distances in homo- and hetero-complexes of orthogonally spin-labeled proteins.

1 Introduction

1.1 DEER

Double Electron-Electron Resonance (DEER, also known as PELDOR) is an electron paramagnetic resonance (EPR) pulsed dipolar spectroscopy (PDS) technique introduced by Milov et al. (Milov et al., 1981, 1984) and further developed by Spiess and Jeschke (Martin et al., 1998; Pannier et al., 2000) that probes the r^{-3}-dependent dipolar coupling interaction between adjacent unpaired electron spins. DEER allows the extraction of precise distance information from 1.5 nm to about 8 nm on spin-labeled proteins in partially deuterated solvents and is an established technique in structural biology (Jeschke, 2012, 2018), complementary to X-ray crystallography, NMR spectroscopy and cryo electron microscopy. Perspectively, it is also seen among the most promising methods for in-cell studies (Plitzko et al., 2017).

DEER is usually performed using the dead-time free 4-pulse DEER sequence (Martin et al., 1998; Pannier et al., 2000), a two frequency experiment that allows detecting the dipolar modulation of the observer echo induced by changing the position of

https://doi.org/10.5194/mr-2020-15
Preprint. Discussion started: 23 June 2020


Open Access MAGNETIC RESONANCE Discussions

the pump pulse within the dipolar evolution time. There are two contributions to the time trace: an inter-molecular background function that needs to be fitted and separated from the intra-molecular, desired signal.

A reliable fit of the background function relies on recording the primary DEER time trace as long as possible, so that the last 2/3 of the trace contains a pure background decay function. This is usually difficult to experimentally achieve for distances $>$ 5-6 nm, especially for samples carrying low concentrations of fast relaxing spins, as it is the case e.g. for spin-labeled membrane proteins. Decreasing the spin concentration alleviates the background problem, because at concentrations $<$ 10 µM the background is an almost flat function, which is easier to be fitted and removed from the trace. Ambiguous background fitting can cause large uncertainties in distance distributions, that can be quantified by data validation approaches in DeerAnalysis (Jeschke et al., 2006).

Dividing the primary DEER time trace by the fitted background function results in the form factor that can be fitted using several approaches, most prominently Tikhonov regularization (Chiang et al., 2005; Jeschke et al., 2006) or Gaussian fitting, yielding the distance distribution between intra-molecular dipolarly coupled spins. The recently introduced neural network analysis of DEER data (Worswick et al., 2018) allows direct analysis of primary DEER time traces, providing distance distributions with an uncertainty estimate based on variations in the fits of multiple networks.

1.2 Orthogonal labeling

In multispin systems carrying the same type of spin label, the assignment of distances within the overall distance distribution can be challenging due to the presence of ghost peaks (von Hagens et al., 2013) and the intrinsic difficulties in disentangling multiple distance contributions, often already when only three spin labels are present in the system (Jeschke et al., 2009; Pribitzer et al., 2017). However, the analysis is simplified for oligomeric systems with a defined symmetry (Valera et al., 2016).

Orthogonal spin labeling (Yulikov, 2015) facilitates the assignment of distances via selectively addressable DEER channels that give access to distance information of specific spin pairs at a time thereby increasing the information content that can be obtained from a single sample. The term orthogonal refers to spin labels that are spectroscopically distinguishable from each other and can be addressed and/or detected independently, e.g. via distinct resonance frequencies, relaxation behavior or transition moments.

Two orthogonal spin labels in a system give access to three DEER channels: two channels probing the interactions between two labels of the same type and one channel probing interactions between two different labels. Depending on the system under study, signals can appear in none, one, two or all three DEER channels. In case of a spectral overlap between the orthogonal labels (which is commonly the case when nitroxides are used in combination with metal ions), crosstalk signals between the DEER channels might appear depending on the degree of orthogonality between the labels and their relative abundance within the sample. This topic has been touched in the literature before (Gmeiner et al., 2017; Teucher et al., 2019) but was never thoroughly investigated.

DEER experiments have already been performed on a large number of combinations of orthogonal spin labels, e.g. nitroxides in combination with trityl (Shevelev et al., 2015; Joseph et al., 2016; Jassoy et al., 2017), Gd^{III} (Lueders et al., 2011, 2013;

https://doi.org/10.5194/mr-2020-15
Preprint. Discussion started: 23 June 2020

Open Access MAGNETIC RESONANCE Discussions

Garbuio et al., 2013; Kaminker et al., 2013), Fe^{III} (Ezhevskaya et al., 2013; Abdullin et al., 2015; Motion et al., 2016), Cu^{II} (Narr et al., 2002; Meyer et al., 2016) or Mn^{II} (Kaminker et al., 2015; Akhmetzyanov et al., 2015; Meyer and Schiemann, 2016).

1.3 Combination of nitroxide and gadolinium^{III}

Nitroxides (NO) and Gd^{III}-based spin labels (Gd) are the most commonly used orthogonal spins for DEER experiments on biomolecules. Nitroxides are $S = 1/2$ spin systems with a spectral width in the order of 10 mT at Q band ($\approx$ 35 GHz). Gd^{III}-based spin labels are $S = 7/2$ systems extending over 450 mT at Q band with a sharp central $|-1/2\rangle \rightarrow |+1/2\rangle$ transition whose maximum is usually about 10.4 mT ($\approx$ 291 MHz) higher in magnetic field than the maximum of the NO spectrum. Furthermore, the transition moments and the relaxation behavior of the two spin probes are very distinct allowing for a selective addressability in pulsed EPR experiments. In particular, a π-pulse for NO corresponds to a 4 π-pulse for the $|-1/2\rangle \rightarrow |+1/2\rangle$ transition of Gd (Yulikov, 2015) which stands for a 12 dB difference in applied microwave power. Another relevant difference between NO and Gd are their distinct T_1 and T_2 relaxation times, which can be used to filter for NO and Gd signals in the DEER observer channel by changing the shot repetition time and the length of the dipolar evolution time, respectively.

In this work, we focus on orthogonal DEER experiments performed at Q band using NO and Gd spin labels. These two spin probes give access to three DEER channels, hereafter referred to as: NONO, NOGd and GdGd. We chose three rulers, namely an NO-NO, an NO-Gd and a Gd-Gd ruler with distinct non-overlapping distance distributions to study in a systematic way the signals arising in all detectable DEER channels if one, two or three different rulers are present in the same sample.We identified distance combinations and DEER channels that are prone to crosstalk signals and quantified their relative strengths thereby providing suggestions on how to identify and suppress their contributions.

2 Materials and methods

2.1 Samples

Here, the Gd-Gd ruler Na_2[{Gd^{III}(PyMTA)}-$(EP)_5$E-{Gd^{III}(PyMTA)}] (Qi et al., 2016a), the NO-Gd ruler Na[{Gd^{III}(PyMTA)}-$(EP)_2$-NO•] (Ritsch et al., 2019), and the NO-NO ruler NO•-$(EP)_2$P-NO•, were used (for structural formulae see Fig. 1). In these compounds two {Gd^{III}(PyMTA)} (Qi et al., 2016b) complexes, a {Gd^{III}(PyMTA)} complex and a nitroxide, and two nitroxides are held at a distance of 4.7 nm, 2.5 nm, and 2.0 nm, respectively, by a rod-like spacer. Because of their geometry and the rather high stiffness of the spacer (Jeschke et al., 2010) their interspin distances are well-defined. All rulers are water soluble and can therefore be detected in the same environment as water soluble proteins. The synthesis and characterization of the Gd-Gd and the NO-Gd rulers was published before (Qi et al., 2016a; Ritsch et al., 2019), while the synthesis of the water soluble NO-NO ruler is described in the SI Part A.

The samples were prepared using stock solutions of the rulers in H_2O at concentrations of 50 - 100 µM. To each sample 50% v/v deuterated glycerol was added as cryoprotectant yielding the final spin concentrations given in Table S1 (SI Part B). 40 µl of each sample were inserted into 3 mm outer diameter quartz tubes and shock frozen in liquid nitrogen.

https://doi.org/10.5194/mr-2020-15
Preprint. Discussion started: 23 June 2020

Open Access MAGNETIC RESONANCE Discussions

2.2 Instrumentation

2.2.1 Spectrometer

Continous wave (cw) EPR experiments for NO spin counting were performed at X band using a MiniScope MS 5000 spectrometer (Magnettech by Freiberg Instruments). All pulsed EPR experiments were performed using a Bruker Biospin Q-band Elexsys E580 spectrometer equipped with a 150 W TWT amplifier from Applied Systems Engineering and a Bruker SpinJet-AWG (±400 MHz bandwidth, 1.6 GSa/s sampling rate, 14 bit amplitude resolution) in combination with a home-made Q-band resonator for 3 mm sample tubes (Tschaggelar et al., 2009; Polyhach et al., 2012).

2.2.2 Pulse parameters

All pulse experiments were performed using monochromatic pulses with a Gaussian amplitude modulation function, predefined as pulse shape 1 in Bruker Xepr 2.6b.119. In Xepr, the pulse length t_p of a Gaussian pulse is defined as its time base (truncation at 2.2% of its maximum amplitude) which is related to its full width at half maximum (FWHM) by $t_p = 2\sqrt{2ln2} \cdot \mathrm{FWHM} \approx 2.3548 \cdot \mathrm{FWHM}$ (Teucher and Bordignon, 2018).

2.2.3 DEER setup

DEER experiments were performed using the dead-time free 4-pulse DEER sequence $(\pi/2)_{obs} - (d_1) - (\pi)_{obs} - (d_1{+}T) - (\pi)_{pump} - (d_2{-}T) - (\pi)_{obs} - (d_2) - (\mathrm{echo})$ (Martin et al., 1998; Pannier et al., 2000) with 16-step phase cycling (Tait and Stoll, 2016) using (0)-(π) for $(\pi/2)_{obs}$ and $(\pi)_{obs}$, and (0)-(π/2)-(π)-(3π/2) for $(\pi)_{pump}$. Gaussian π/2- and π-pulses at the observer frequency were created by varying the pulse amplitude at a fixed pulse length to maintain a uniform excitation bandwidth for the refocused echo (Teucher and Bordignon, 2018). The length of the pulses was optimized via transient nutation experiments for each spin type as shown in Fig. 2. The main frequency of the microwave bridge was set to the observer position with the AWG

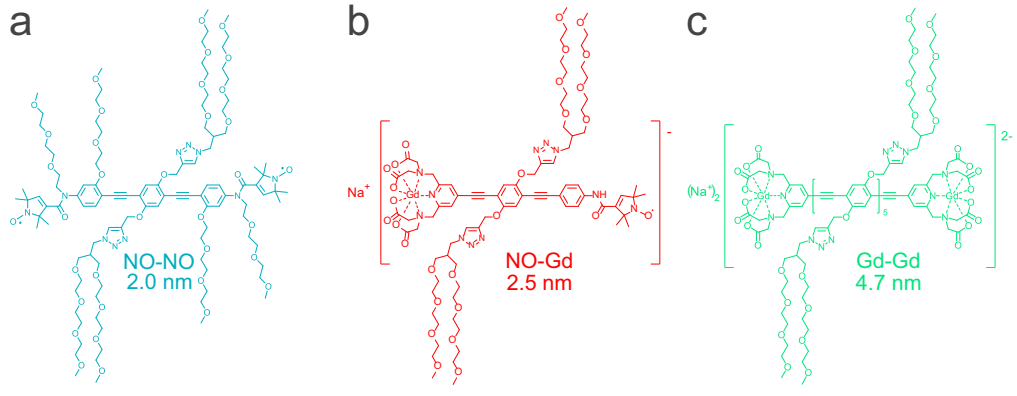

Figure 1. Structural formulae of the NO-NO, NO-Gd and Gd-Gd rulers. Indicated are the experimentally detected mean distances between the paramagnetic centers.

https://doi.org/10.5194/mr-2020-15
Preprint. Discussion started: 23 June 2020

Open Access MAGNETIC RESONANCE Discussions

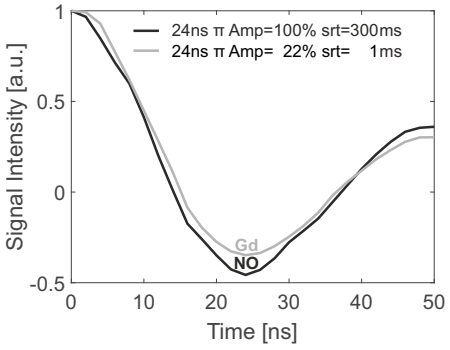

Figure 2. NO and Gd nutation experiments. Transient nutation experiments performed at 10 K with different shot repetition times (srt) and pulse amplitudes within the spectral overlap of NO and Gd (at the maximum of the NO signal). Based on the different longitudinal relaxation times of the two spin probes, srt filtering allows independent addressability. Adjusting the pulse amplitudes allows matching the π-pulse lengths of NO and Gd. At an srt of 300 ms the predominant nutation signal contribution arises from the NO which has in the center of the dip at 100% AWG amplitude a 24 ns (10.2 ns FWHM) Gaussian π-pulse length. Decreasing the srt from 300 ms to 1 ms allows filtering for Gd, which matches the 24 ns π-pulse length at 22% AWG amplitude. This difference in AWG amplitude corresponds to a 12 dB difference in power between NO and Gd (Yulikov, 2015) based on their distinct transition moments.

synthesizing the frequency offset required for the pump pulse. More details about the DEER setups for the orthogonal spin probes are given in Fig. 3. The evaluation of the DEER data was performed using the Gaussian fitting routine of DeerAnalysis2019 (Jeschke et al., 2006). Gaussian fitting was chosen over Tikhonov regularization since it simplifies data evaluation for well-defined narrow distance distributions as it is the case for the rulers. In particular, it allows simultaneous fitting of components with very different distribution widths as required for the utilized samples. A side-by-side comparison of both methods is presented in Fig. S1 (SI Part B).

https://doi.org/10.5194/mr-2020-15
Preprint. Discussion started: 23 June 2020

Open Access MAGNETIC RESONANCE Discussions

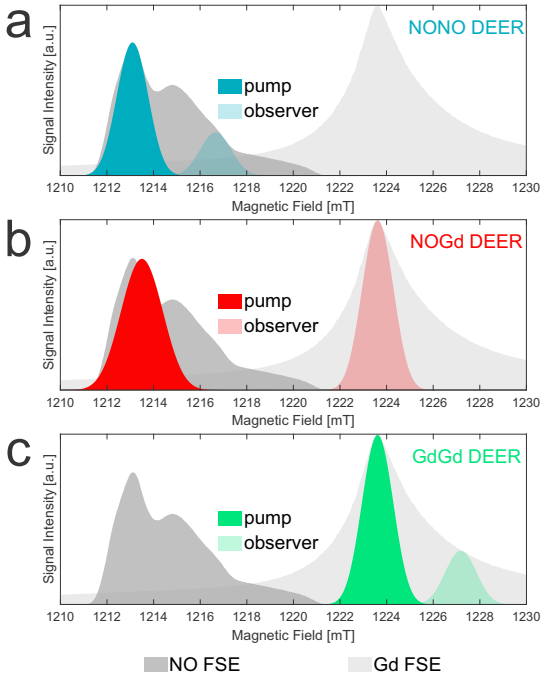

Figure 3. Three channel DEER setups. NO and Gd field-swept echo (FSE) spectra are shown as shaded gray areas with overlaid Gaussian pump and observer π-pulse excitation profiles simulated with EasySpin 5.2.2 (Stoll and Schweiger, 2006). In all setups, Gaussian observer pulses of 32 ns time base length (13.6 ns FWHM) (Teucher and Bordignon, 2018) were used in combination with a shot repetition time (srt) of 1000 µs. (a) NONO DEER: 32 ns Gaussian pump on spectral maximum of NO; observer pulses 100 MHz lower in frequency; pump/observer placed symmetrical in resonator profile; performed at 50 K. (b) NOGd DEER: 24 ns (10.2 ns FWHM) Gaussian pump placed in the center of the resonator profile; pump position 0.4 mT higher in field than the spectral maximum of NO with observer 280 MHz lower in frequency on spectral maximum of Gd; performed at 10 K. (c) GdGd DEER: as in (a), except for the pump pulse placed on the maximum of the Gd spectrum; performed at 10 K.

https://doi.org/10.5194/mr-2020-15
Preprint. Discussion started: 23 June 2020

Open Access MAGNETIC RESONANCE Discussions

3 Experimental results and discussion

3.1 Isolated rulers

The DEER characterization of the three individual rulers is shown in Fig. 4. Since both the NO-NO and the Gd-Gd rulers contain only one type of label, we could probe per sample only one DEER channel, namely the NONO or GdGd channel, respectively, whereas the orthogonally labeled NO-Gd ruler gives access to all three DEER channels. Notably, the obtained dipolar frequencies and modulation depths of the isolated ruler samples with their corresponding distance distributions are characteristic sample- and setup-dependent parameters which will be used in the following to identify and quantify crosstalk signals in the ruler mixtures.

The NONO DEER time trace (blue) detected on the NO-NO ruler in Fig. 4(a) shows a dipolar frequency characterized by a 35% modulation depth, corresponding to a well-defined 2 nm distance. The GdGd DEER time trace (green) detected on the Gd-Gd ruler shows a dipolar frequency with a modulation depth of $\approx 3\%$, corresponding to a monomodal distance distribution centered at 4.7 nm (see Fig. 4(b)).

The time traces obtained on the NO-Gd ruler with the three DEER channels are shown in Fig. 4(c). The NOGd DEER time trace (red) shows a defined dipolar frequency which is characterized by a 30% modulation depth and correlates with a 2.5 nm distance. Unexpectedly, the NONO DEER channel (blue) also contains a dipolar signal whose distance distribution coincides with the one obtained in the NOGd DEER channel. In contrast, the GdGd channel (green) contains a mere background function. The absence of a dipolar modulation in the GdGd DEER channel proves that the NO-Gd ruler is monomeric in solution. Therefore, we can conclude that the signal detected in the NONO DEER channel is a crosstalk signal. This crosstalk signal originates from a residual excitation of the Gd spectrum overlapping with the nitroxide spectrum by the pump and/or observer pulses in the NONO DEER sequence. This crosstalk signal is significant, because its $\approx 4\%$ modulation depth is in the order of 10% of the maximally achievable modulation depth for the spin-labeled NO-NO ruler (see Fig. 4(a)). We classify this signal as a NO-Gd crosstalk in the NONO DEER channel and designate it as $\mathbf{X}_1$.

3.2 Ruler mixtures

In this section we investigate the appearance of crosstalk signals between the DEER channels in samples containing pairwise mixtures of the three rulers. The data are presented in Fig. 5.

The three DEER experiments performed on the mixture of the NO-NO ruler with the NO-Gd ruler in a 1:1 molar ratio are shown in Fig. 5(a). The NONO DEER channel contains the expected distance distribution of the isolated NO-NO ruler characterized in Fig. 4(a) with a slightly smaller modulation depth. The NOGd channel reproduces the signal obtained on the isolated NO-Gd ruler previously shown in Fig. 4(b). The GdGd channel shows no dipolar modulation, in line with the absence of Gd-Gd rulers in this sample.

The NO-Gd crosstalk signal in the NONO channel ($\mathbf{X}_1$) detected for the isolated NO-Gd ruler in Fig. 4(c) would be theoretically expected at 2.5 nm. Interestingly, this signal is not experimentally resolved in the mixture of NO-NO ruler with NO-Gd ruler. As addressed before, this crosstalk signal is caused by a residual excitation of Gd spins via the NO-optimized pump and/or

https://doi.org/10.5194/mr-2020-15
Preprint. Discussion started: 23 June 2020

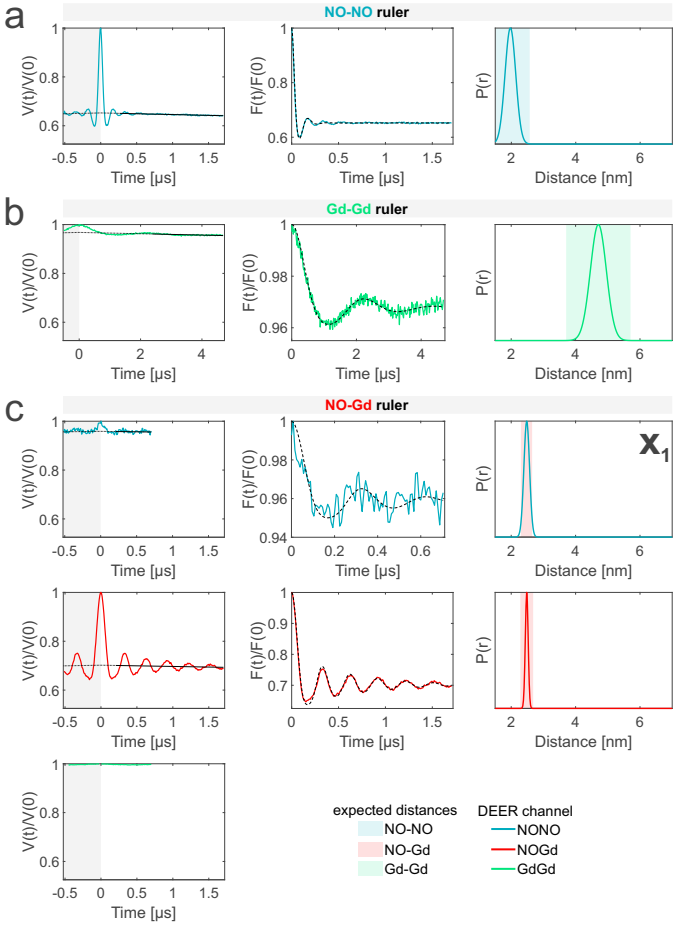

Figure 4. Characterization of the isolated rulers. The DEER setups are introduced in Fig. 3. Left, primary data with background fit (gray areas are excluded from data evaluation); middle, form factors with Gaussian fit; right, obtained distance distributions. A Tikhonov analysis of the data is shown in Fig. S1 (SI Part B). The time traces, form factors and distance distributions recorded with the NONO DEER channel are colored in blue, those recorded with the GdGd channel are green, and those recorded with the NOGd channel are red. Regions in which distances can be theoretically expected based on the rulers present in the specific sample are represented as shaded blue, green and red areas in the distance distributions. "$\mathbf{X}_1$" is an NO-Gd crosstalk in the NONO DEER channel.

observer pulses. When considering that the pump pulse excites the Gd spins, and the observer excites the NO spins of the NO-Gd ruler, one needs to take into account that in this sample, only 1/3 of the NO observer signal in the NONO channel originates from the NO-Gd ruler, which would decrease the modulation depth of the crosstalk signal from the 4% detected on the isolated NO-Gd ruler (see Fig. 4(c)), to 1% for this sample, which is hardly detectable. When considering that the NO-optimized observer pulse excites the residual Gd spins of the NO-Gd ruler, one has to consider that the overall observer echo has a predominant NO contribution and therefore an even lower modulation depth is expected. Accordingly, we suggest that the dominant signal contribution at 2 nm arising from the NO-NO ruler masks the NO-Gd crosstalk signal.

https://doi.org/10.5194/mr-2020-15
Preprint. Discussion started: 23 June 2020

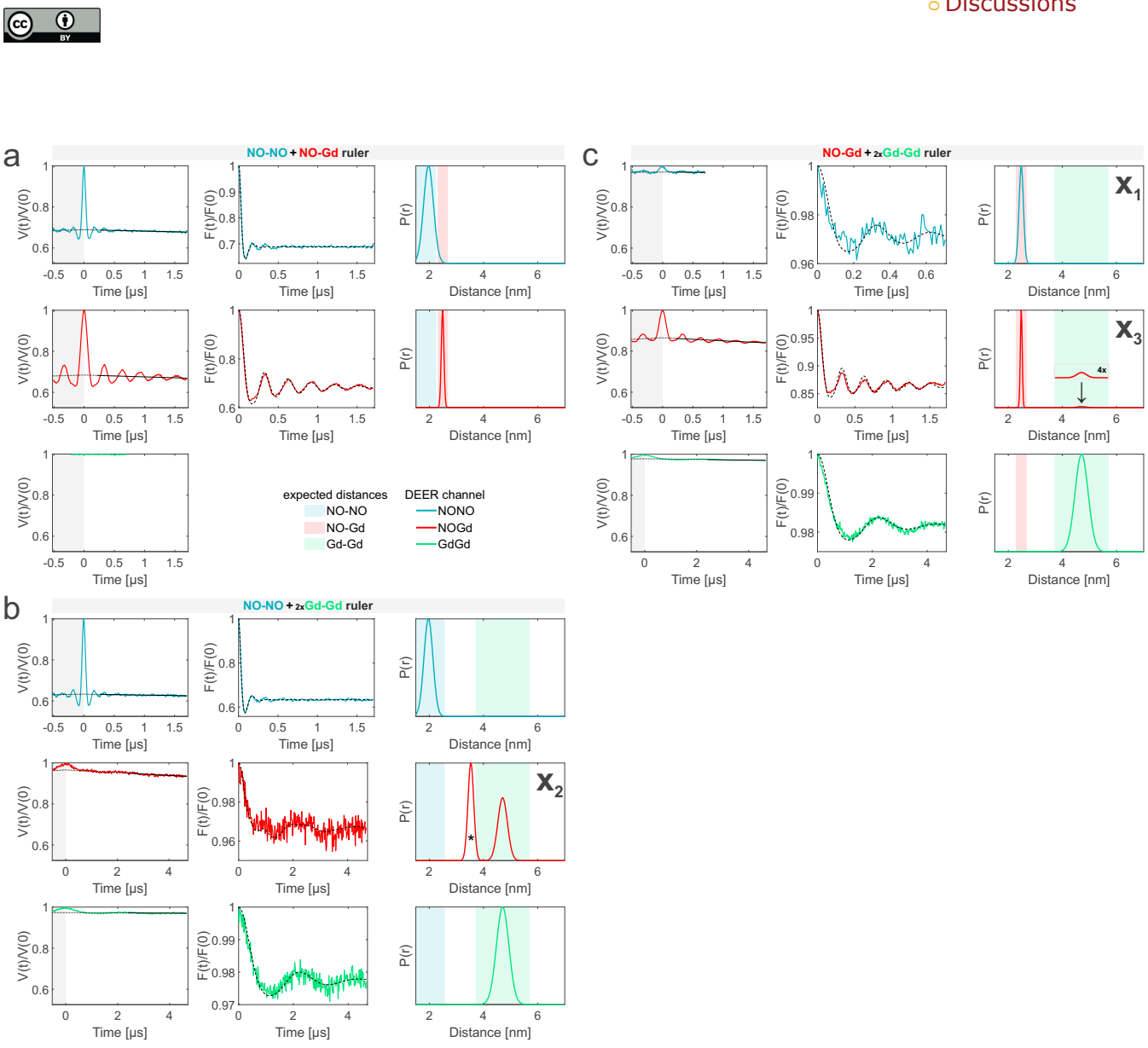

Figure 5. Pairwise mixtures of rulers. The DEER setups are introduced in Fig. 3. Left, primary data with background fit (gray areas are excluded from data evaluation); middle, form factors with Gaussian fit; right, obtained distance distributions. Color coding as in Fig. 4. (a) Sample containing the NO-NO and the NO-Gd rulers mixed in a 1:1 molar ratio. (b) Sample containing the NO-NO and the Gd-Gd rulers mixed in a 1:2 ratio. The NOGd DEER channel contains a Gd-Gd crosstalk signal $\mathbf{X}_2$. The distance indicated with an asterisk originates from a spectrometer-specific artifact signal. (c) Mixture of the NO-Gd ruler with the Gd-Gd ruler in a 1:2 ratio. NO-Gd crosstalk signal in the NONO channel ($\mathbf{X}_1$) and Gd-Gd crosstalk signal in the NOGd channel in presence of an NO-Gd signal ($\mathbf{X}_3$).

The analysis of the sample containing the NO-NO ruler and the Gd-Gd ruler in a 1:2 molar ratio is presented in Fig. 5(b). Both the NONO and the GdGd channels reproduce nicely the DEER signals obtained on the isolated NO-NO and Gd-Gd rulers. As there is no NO-Gd ruler present in the sample, no signal would be expected in the respective DEER channel. Indeed, no NO-Gd distance was detected but, instead, a Gd-Gd crosstalk signal was visible in the NOGd channel (defined as $\mathbf{X}_2$). Apart

https://doi.org/10.5194/mr-2020-15
Preprint. Discussion started: 23 June 2020

Open Access MAGNETIC RESONANCE Discussions

from that, the NOGd channel contains a secondary 3.5 nm distance which originates from a spectrometer-specific oscillatory signal of constant amplitude present in the time domain trace which is discussed in more detail in section 3.3. The modulation amplitude of this spectrometer artifact adds up to the modulation depth of the Gd-Gd crosstalk signal. The actual crosstalk signal has a modulation depth of about 3% which is (as in the case of the NO-Gd crosstalk in the NONO channel, defined as $\mathbf{X}_1$) in the order of 10% of the maximally expected modulation depth of 30% in this channel (see Fig. 4(c)) and therefore non-negligible.

The results of the experiments with the 1:2 mixture of the NO-Gd ruler with the Gd-Gd ruler are presented in Fig. 5(c). The NONO DEER channel of this sample shows the NO-Gd crosstalk signal ($\mathbf{X}_1$) as reported for the isolated NO-Gd ruler in Fig. 4(c). The identification of this crosstalk signal is facilitated by the absence of a real NO-NO distance. The GdGd channel, due to the absence of any spectral overlap in our DEER setup, is intrinsically artifact-free and shows the expected pure Gd-Gd distance. In contrast, the NOGd channel contains, besides the expected NO-Gd distance, a Gd-Gd crosstalk signal defined as $\mathbf{X}_3$ which is not fully resolved in the 1.7 µs time trace presented in Fig. 5(c). However, it is clearly visible in a longer time trace presented in section 3.3. $\mathbf{X}_2$ in Fig. 5(b) and $\mathbf{X}_3$ in Fig. 5(c) are both Gd-Gd crosstalk signals in the NOGd channel, however, we decided to keep a distinction in the names based on the absence/presence of a "real" NO-Gd distance which will have an influence on the identification procedure discussed below.

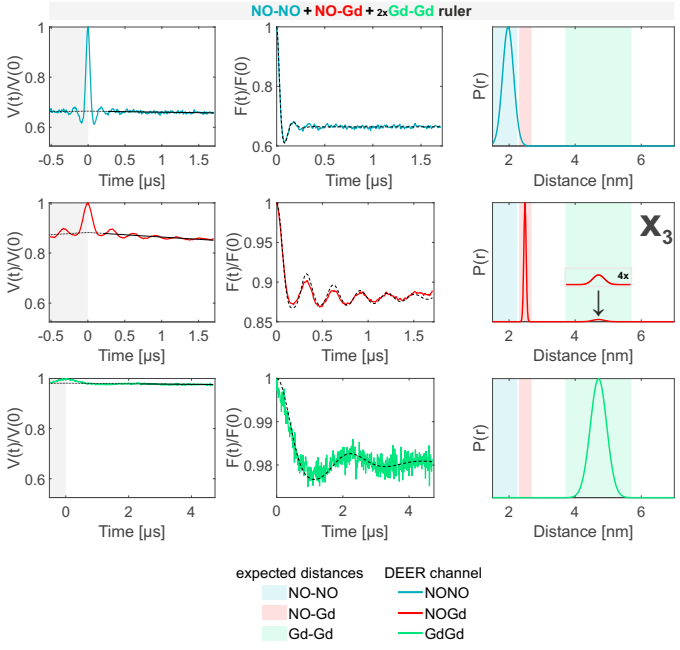

Figure 6. Mixture of NO-NO, NO-Gd and Gd-Gd rulers in a 1:1:2 ratio. The DEER setup is introduced in Fig. 3. Left, primary data with background fit (gray areas are excluded from data evaluation); middle, form factors with Gaussian fit; right, obtained distance distributions. Color coding as in Fig. 4. "$\mathbf{X}_3$" is a Gd-Gd crosstalk signals in the NOGd channel.

https://doi.org/10.5194/mr-2020-15
Preprint. Discussion started: 23 June 2020


Open Access MAGNETIC RESONANCE Discussions

The DEER data obtained on the sample containing the NO-NO, NO-Gd and Gd-Gd rulers in a 1:1:2 ratio are presented in Fig. 6. Essentially, these data can be seen as a superposition of the data detected on the pairwise mixtures of rulers. The NONO DEER channel shows the distance distribution of the NO-NO ruler but lacks the $\mathbf{X}_1$ crosstalk signal because it is masked by the intensity of the NO-NO DEER signal. Besides the expected NO-Gd ruler distance, the NOGd channel shows the Gd-Gd crosstalk signal $\mathbf{X}_3$ as in Fig. 5(c), which is clearly visible in the asymmetry of the time trace due to the underlying low frequency Gd-Gd signal. Finally, the GdGd DEER channel resolves the Gd-Gd distance free of crosstalk signals.

In conclusion, we identified three non-negligible crosstalk signals in the NONO and NOGd DEER channels and we showed that the GdGd DEER setup with the observer frequency placed on the maximum of the Gd signal and the pump frequency at the high field edge of the Gd spectrum (Fig. 3(c)) is intrinsically crosstalk-free in all experimental conditions tested.

3.3 DEER channel crosstalk identification and suppression

The DEER channel crosstalk signals discussed in this work are named as follows: $\mathbf{X}_1$ is an NO-Gd crosstalk signal in the NONO channel, while $\mathbf{X}_2$ and $\mathbf{X}_3$ are both Gd-Gd crosstalk signals in the NOGd channel but in the absence or presence of a "real" NO-Gd signal, respectively. An overview of all crosstalk signals that can be theoretically expected versus those that were experimentally detected using our samples and experimental setups is presented in Table S2 (SI Part B). The origin of all crosstalk signals reported in this work is the spectral overlap between NO and Gd illustrated in Fig. 3(b), which does not allow a completely independent addressability.

The NO-Gd crosstalk signal in the NONO channel $\mathbf{X}_1$ is unavoidable when probing the NONO DEER channel at Q band (see Fig. 3(a)) in presence of a NO-Gd distance. There are two possible origins for this crosstalk signal of the NO-Gd ruler: i) the observer pulses selectively excite the NO and the pump pulse excites the NO and sub-optimally the coupled Gd spins; ii) the observer pulses excite the NO and sub-optimally the Gd while the pump pulse selectively excites the coupled NO spins. To test the effect of the pump pulse on the crosstalk signal, we decreased its power by 12 dB in order to optimize the pump π-pulse for the Gd spins. This resulted only in a small decrease in the modulation depth of the crosstalk signal (data not shown) which implies that there are contributions of Gd spins both in the pump and in the observer echo at the same time. Subsequently, both possibilities discussed above occur simultaneously. We could not find a strategy to minimize this crosstalk signal in the NONO channel, however, if a real NO-NO distance is present, the contribution of this unwanted signal was found to be negligible (see Fig. 5(a)).

We focus now on the $\mathbf{X}_3$ crosstalk signal (Gd-Gd crosstalk in the NOGd channel in the presence of a real NO-Gd distance) from Fig. 5(c). In Fig. 7(a) we present a long NOGd DEER time trace (red) detected on the sample from Fig. 5(c). The two distinct dipolar frequencies of the NO-Gd (high frequency) and Gd-Gd (low frequency) rulers are clearly visible in the primary data. The distance analysis of this time trace using two Gaussians reveals both an NO-Gd distance peak and a Gd-Gd crosstalk distance peak. Since in the NOGd DEER channel, NO is pumped and Gd is observed (see Fig. 3(b)), the observer pulses excite only Gd spins, therefore, the Gd-Gd crosstalk signal originates from sub-optimally pumping the Gd at the NO position due to the spectral overlap. Decreasing the pump pulse power by 12 dB from optimally pumping the NO with a π-pulse to optimally pumping the Gd with a π-pulse (dark red in Fig. 7(a)) strongly decreases the modulation depth (from 15% to 2%; $\approx$ 1/7x) and

https://doi.org/10.5194/mr-2020-15
Preprint. Discussion started: 23 June 2020

Open Access MAGNETIC RESONANCE Discussions

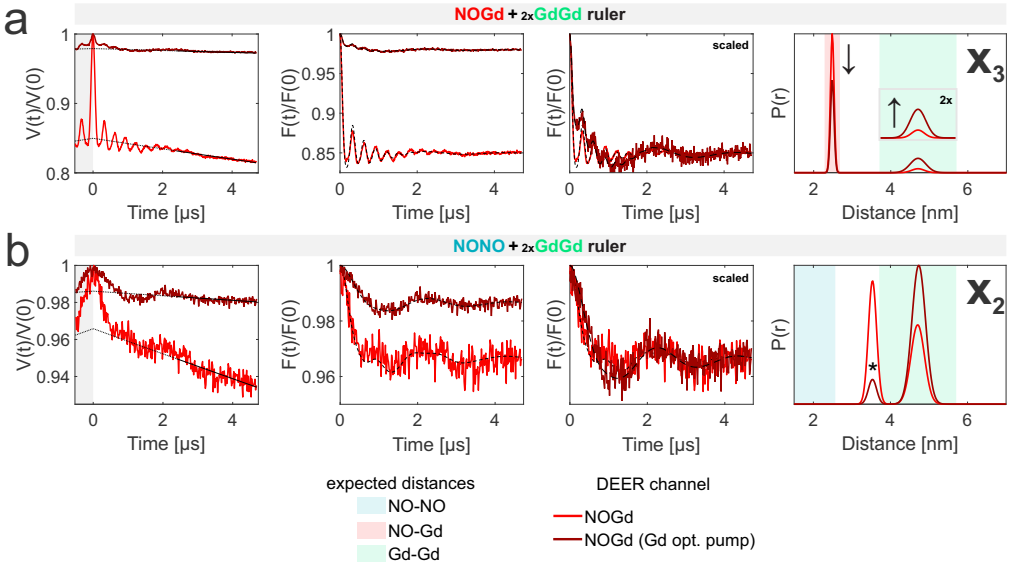

Figure 7. Crosstalk signal identification. Left, primary data with background fit (gray areas are excluded from data evaluation); middle, form factors with Gaussian fit (original data and modulation depth scaled data); right, obtained distance distributions. Color coding as in Fig. 4. In the NOGd DEER setup, NO is pumped and Gd is observed as illustrated in Fig. 3(b). Both $\mathbf{X}_2$ and $\mathbf{X}_3$ crosstalk signals arise from a partial excitation of the underlying Gd at the NO position in an NOGd DEER. (a) and (b) show how decreasing the pump pulse power from optimally pumping NO (red) to optimally pumping Gd (-12 dB, dark red) changes the signal-to-crosstalk ratio and thereby allowing the identification of the crosstalk signal. The relative change in modulation depth is considerably larger if a "real" NO-Gd signal is present together with the crosstalk signal ($\approx$ 1/7x for $\mathbf{X}_3$ versus $\leq$ 1/2x for $\mathbf{X}_2$). The 3.5 nm distance marked with an asterisk originates from a spectrometer-specific artifact.

changes the ratio of the two distance peaks in favor of the crosstalk distance, as expected (see inset). The decrease in power of the pump pulse allows the identification of the $\mathbf{X}_3$-crosstalk signal since optimally pumping the Gd promotes the intensity of the Gd-Gd crosstalk distance (see next paragraph for additional information) while strongly decreasing the intensity of the NO-Gd distance. It is important to note that also the Gd-optimized pump pulse still partially pumps the NO and therefore the DEER trace contains a residual NO-Gd signal contribution.

In Fig. 7(b) the same approach is used to identify the Gd-Gd crosstalk signal in the NOGd channel in the absence of a NO-Gd signal ($\mathbf{X}_2$) (see Fig. 5(b)). The NO-Gd signal (red) is a superposition of the Gd-Gd crosstalk signal corresponding to a distance centered at 4.7 nm and an additional 3.5 nm distance originating from a spectrometer-specific artifact. Decreasing the pump pulse power by 12 dB to optimally pumping the Gd (dark red) considerably suppresses the spectrometer-specific artifact contribution while slightly decreasing the main Gd-Gd dipolar modulation. The modulation depth contribution of the Gd-Gd signal in this setup is about 1.25%, which is in line with the modulation depth obtained with the same setup on the isolated Gd-Gd ruler shown in Fig. S2 (SI Part B). Therefore, we found that by changing the pump power by 12 dB to optimize the inversion pulse for the Gd spins, the modulation depth of the Gd-Gd signal slightly decreases. We can conclude that if there is

https://doi.org/10.5194/mr-2020-15
Preprint. Discussion started: 23 June 2020

Open Access MAGNETIC RESONANCE Discussions

a Gd-Gd crosstalk signal in the NOGd channel in the absence of a real NO-Gd signal, decreasing the pump power by 12 dB produces a small change in modulation depth ($\leq$ 1/2x). This makes it possible to identify an $\mathbf{X}_2$ crosstalk signal. In contrast, if a real NO-Gd distance is present, as in the case of the $\mathbf{X}_3$ crosstalk signal in Fig. 7(a), the overall modulation depth largely decreases (to $\approx$ 1/7x) and the ratio of the distance peaks in the overall distance distribution changes in favor of the crosstalk peak, which can be identified.

To actually suppress crosstalk signals in the overall distance distribution, swapping the pump and observer positions in the NOGd channel could be an option. Usually we pump the NO and observe the Gd spins (see Fig. 3(b)) to optimize the modulation depth in the NOGd channel. In this setup, the observer echo is solely created by the Gd spins. Therefore, crosstalk signals are caused by the pump pulse which is optimized to selectively address NO spins but also partially excites Gd spins. If the positions of pump and observer pulses are swapped, the observer pulses will be placed in the spectral overlap, while the pump pulse will excite only Gd spins. The advantage of the latter approach is that the observer sequence being composed of three pulses can act as a better filter for one spin species than a single pump pulse. This is illustrated in Fig. 8 where field-swept echo experiments were performed at different pulse amplitudes using the refocused echo created by the DEER observer sequence (in absence of the pump pulse). At 100% pulse amplitude, the pulses are optimal $\pi/2$- and π-pulses for the NO, but strongly over-flipping the Gd spins, for which optimal π-pulses require an amplitude of approximately 14% (both determined via transient nutation experiments, data not shown). By lowering the pulse amplitude of the observer pulses to 50%, it is possible to favor even more the intensity of the NO spins in the refocused echo with respect to the Gd spins, therefore increasing the selectivity of the observer sequence towards the wanted NO spins and suppressing the Gd contribution. Using these pulse amplitudes in the observer sequence should maximize the wanted NO-Gd signal, while minimizing the unwanted Gd-Gd crosstalk signal. The main disadvantage of this approach is that very long shot repetition times are required to observe

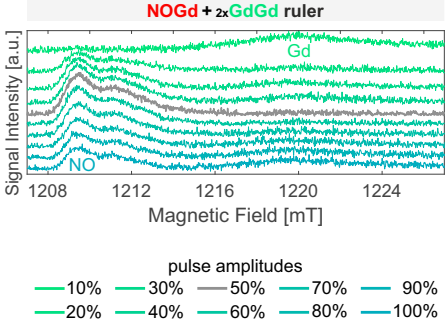

Figure 8. Crosstalk signal suppression. The absolute values of the complex FSE spectra detected using a refocused Hahn echo sequence (DEER observer sequence) on the 1:2 mixture of the NO-Gd and Gd-Gd ruler are shown. The experiments were performed at 10 K with a shot repetition time of 100 ms (filtering for the NO, see Fig. 2). With respect to the standard NOGd DEER setup shown in Fig. 3(b), the positions of pump and observer pulses were exchanged. The observer was placed at a frequency where 100% pulse amplitude corresponds to a π-pulse on the NO. Due to the distinct transition moments of NO and Gd, the relative intensities of the spectral contributions change when varying the pulse amplitudes. At 50% amplitude only the NO spectrum is refocused.

https://doi.org/10.5194/mr-2020-15
Preprint. Discussion started: 23 June 2020


Open Access MAGNETIC RESONANCE Discussions

on the NO (100 ms for the NO with respect to 1 ms for Gd in the conventional setup), which makes DEER data acquisition impractically long for this combination of spin labels to achieve a satisfactory signal-to-noise. Additionally, the small fraction of Gd spins excited by a Gaussian pump leads to a small modulation depth for the desired NO-Gd signal. The latter issue could be improved using phase- and amplitude-modulated broadband pump pulses, as it was previously shown as a way to improve modulation depths for Gd spin pairs (Doll et al., 2013; Spindler et al., 2013; Doll et al., 2015; Bahrenberg et al., 2017). Overall, this approach is interesting and might be of use for other pairs of orthogonal spin labels.

4 Conclusions and outlook

In this work we thoroughly investigated the appearance of crosstalk signals between the three possible DEER channels at Q-band frequencies on mixtures of NO-NO, NO-Gd and Gd-Gd rulers with non-overlapping distance distributions. Crosstalk signals in DEER experiments with two types of spin systems had been suspected in the literature before (Gmeiner et al., 2017; Teucher et al., 2019) but could never be unambiguously identified and characterized.

We experimentally detected a NO-Gd crosstalk signal $\mathbf{X}_1$ in the NONO DEER channel in the absence of real NO-NO distances and two Gd-Gd crosstalk signals $\mathbf{X}_2$ or $\mathbf{X}_3$, in the NOGd DEER channel in the absence and presence of a real NO-Gd distance, respectively. We theoretically predicted a fourth crosstalk signal $\mathbf{X}_4$ (see Table S2) which describes a Gd-Gd crosstalk in the NONO channel that was not experimentally detected. This is most likely due to: the low modulation depth that would be expected for this signal based on the non-perfect pump and observer pulses; the long Gd-Gd distance of 4.7 nm of the chosen ruler, which makes it more difficult to identify signals with very low modulation depth; the low spectral density of the Gd at the position of the NO; and the large modulation depth of a real NO-NO signal if present.

Our experimental findings confirm that crosstalk signals can be expected in 4-pulse DEER experiments performed with the observer and/or pump pulses positioned in the region of spectral overlap between NO and Gd spins. Therefore, NONO and NOGd DEER experiments are prone to crosstalk signals, while the GdGd DEER channel with the setup suggested here is intrinsically crosstalk-free (see Fig. 3(c)).

All detected crosstalk signals are of experimental relevance when orthogonally-labeled biomolecular complexes are investigated, since they are in the order of 10% of the maximally expected modulation depth in the respective DEER channel for a doubly spin-labeled protein with 100% labeling efficiency. Signals of this strength are easily resolvable by state-of-the-art high-power Q-band spectrometers (Polyhach et al., 2012) and therefore entail the risk of data misinterpretation when unknown mixtures of orthogonally-labeled proteins are studied. Notably, we found that if a real NO-NO dipolar oscillation with a large modulation depth is present in the NONO channel and the stoichiometric ratio of the different spin types is similar, the possible NO-Gd crosstalk signal is negligible, due to the dominating modulation depth of the real signal (in the order of 30 - 40%) with respect to the expected 1 - 2% of the crosstalk signal.

We were not able to find a spectroscopic approach to identify the NO-Gd crosstalk signal in the NONO channel ($\mathbf{X}_1$), apart from an identification based on the comparison of the distance distributions detected with the NONO and NOGd DEER channels on the same sample, which can be ambiguous. Therefore, if a dipolar oscillation is detected in the NONO DEER

https://doi.org/10.5194/mr-2020-15
Preprint. Discussion started: 23 June 2020


Open Access MAGNETIC RESONANCE Discussions

channel and the obtained distance distribution overlaps with the one detected in the NOGd channel, further analysis is required. To clarify whether a crosstalk signal is detected, we propose to prepare an analogous sample with the Gd-labeled proteins exchanged with the unlabeled variants. If the NONO DEER channel is free of dipolar oscillations, the signal previously detected signal was a crosstalk signal; otherwise, if the same dipolar frequency is detected, then it was a real NO-NO distance.

For the Gd-Gd crosstalk signals in the NOGd DEER channel, which are the most relevant unwanted signals in the analysis of complex protein mixtures, we propose an identification strategy based on decreasing the power of the pump pulse positioned at the maximum of the nitroxide spectrum by 12 dB to optimally pump the Gd spins. This allows to unambiguously identify crosstalk signals $\mathbf{X}_2$ and $\mathbf{X}_3$ via relative changes in their modulation depth. If the overall modulation depth decreases only marginally (maximally to ≈50% of its initial value), the DEER signal is caused by Gd-Gd crosstalk and no real NO-Gd distances are present. In contrast, if the modulation depth decreases to ≈15% of its original value and the primary time trace differs, then the signal is a mixture of a real NO-Gd signal and a Gd-Gd crosstalk signal. In this case, the crosstalk signal is of type $\mathbf{X}_3$ and there must be a relative increase in intensity of the crosstalk signal with respect to the real signal contribution in the distance distribution. This change in relative intensities aids the identification of the crosstalk signal. Notably, the exact values of the relative changes of the modulation depths presented here are valid only in our experimental setup and need to be calibrated for each setup using standard samples. Swapping the position of the pump and observer pulses in the NOGd DEER channel was found to be in principle promising to suppress the NO-Gd crosstalk signal, but experimentally impracticable for samples containing NO and Gd spins due to the prohibitively long shot repetition time of the experiment and the small modulation depths expected. Broadband excitation pump pulses may alleviate the modulation depth issue for spins with large zero field splittings and the long acquisition times would benefit if faster relaxing spin 1/2 labels are used.

It is important to note that the relative strengths of the crosstalk signals depend on the relative molar ratio of the different types of spin labels, as shown by a complete set of experiments performed on an independent set of samples with mixtures of the rulers in equimolar quantities (Table S3 and Fig. S3 to S5, SI Part B). Additionally, other experimental properties such as the relative modulation depths of the real signals and the relative widths of the distance distributions may modulate the relevance of the crosstalk signals in the overall data analysis. Therefore, in this work we identified possible problems arising from crosstalk signals in three DEER channels when using NO and Gd mixtures, but the extent of the crosstalk signals and their relevance on data interpretation depends on the specific properties of the sample under investigation.

Q band currently offers the highest sensitivity to perform the three-channel DEER experiments with samples containing both NO and Gd spin labels on a commercial spectrometer. Gd spin labels would gain in sensitivity at higher frequencies thanks to the narrowing of the spectrum, however, the broadening of the NO spectrum would probably counterbalance these effects in the NONO and NOGd DEER channels. In general, it would be insightful to have a multi-frequency approach and perform these types of experiments at Q- and W-band or higher frequencies to find the best-suited frequency band for each DEER channel- and label- combination. The use of an AWG is advantageous for the proposed identification strategy due to the possibility to use Gaussian pulses (Teucher and Bordignon, 2018), which remove residual “2+1” pulse train signals increasing signal fidelity and to further explore additional benefits of broadband excitation pulses. We did not analyze the effects of multispin systems with more than 2 spins in the mixture, but we can anticipate that appearance of ghost peaks (von Hagens et al., 2013) will

https://doi.org/10.5194/mr-2020-15
Preprint. Discussion started: 23 June 2020


Open Access MAGNETIC RESONANCE Discussions

further complicate data analysis and additional experiments with one type of label removed at a time from the sample should be planned.

Combinations of other orthogonal spin labels with spectral overlap will be also prone to crosstalk signals in DEER and we foresee that the approaches suggested here to identify and possibly suppress unwanted crosstalk signal should be applicable.

Author contributions. MT and EB designed the research. MT prepared the EPR samples and performed all EPR experiments. Compound design and synthesis was contributed by MQ, NC, HH, and AG. MT and EB discussed the results and wrote the manuscript. MQ and AG wrote the SI Part A. The manuscript was revised by all authors.

Competing interests. The authors declare no competing interests.

Acknowledgements. We acknowledge support by Deutsche Forschungsgemeinschaft (DFG, German Research Foundation) under Germany's Excellence Strategy – EXC-2033 – Projektnummer 390677874 (EB), the DFG Priority Program SPP1601 "New Frontiers in Sensitivity in EPR Spectroscopy" [DFG BO 3000/2-1 (EB); DFG GO 555/6-2 (AG)], DFG BO 3000/5-1 (EB), DFG INST 130/972-1 FUGG (EB) and SFB958 – Z04 (EB). The Q-band resonator was kindly gifted by G. Jeschke (ETH Zürich/Switzerland).

https://doi.org/10.5194/mr-2020-15
Preprint. Discussion started: 23 June 2020

Open Access MAGNETIC RESONANCE Discussions

References

Abdullin, D., Duthie, F., Meyer, A., Müller, E. S., Hagelueken, G., and Schiemann, O.: Comparison of PELDOR and RIDME for distance measurements between nitroxides and low–spin Fe (III) ions, J. Phys. Chem. B, 119, 13 534–13 542, 2015.

Akhmetzyanov, D., Plackmeyer, J., Endeward, B., Denysenkov, V., and Prisner, T.: Pulsed electron–electron double resonance spectroscopy between a high-spin Mn2+ ion and a nitroxide spin label, Phys. Chem. Chem. Phys., 17, 6760–6766, 2015.

Bahrenberg, T., Rosenski, Y., Carmieli, R., Zibzener, K., Qi, M., Frydman, V., Godt, A., Goldfarb, D., and Feintuch, A.: Improved sensitivity for W-band Gd (III)-Gd (III) and nitroxide-nitroxide DEER measurements with shaped pulses, J. Magn. Reson., 283, 1–13, 2017.

Chiang, Y.-W., Borbat, P. P., and Freed, J. H.: The determination of pair distance distributions by pulsed ESR using Tikhonov regularization, J. Magn. Reson., 172, 279–295, 2005.

Doll, A., Pribitzer, S., Tschaggelar, R., and Jeschke, G.: Adiabatic and fast passage ultra-wideband inversion in pulsed EPR, J. Magn. Reson., 230, 27–39, 2013.

Doll, A., Qi, M., Wili, N., Pribitzer, S., Godt, A., and Jeschke, G.: Gd (III)–Gd (III) distance measurements with chirp pump pulses, J. Magn. Reson., 259, 153–162, 2015.

Ezhevskaya, M., Bordignon, E., Polyhach, Y., Moens, L., Dewilde, S., Jeschke, G., and Van Doorslaer, S.: Distance determination between low-spin ferric haem and nitroxide spin label using DEER: the neuroglobin case, Mol. Phys., 111, 2855–2864, 2013.

Garbuio, L., Bordignon, E., Brooks, E. K., Hubbell, W. L., Jeschke, G., and Yulikov, M.: Orthogonal Spin Labeling and Gd (III)–nitroxide distance measurements on bacteriophage T4-lysozyme, J. Phys. Chem. B, 117, 3145–3153, 2013.

Gmeiner, C., Dorn, G., Allain, F. H., Jeschke, G., and Yulikov, M.: Spin labelling for integrative structure modelling: A case study of the polypyrimidine-tract binding protein 1 domains in complexes with short rnas, Phys. Chem. Chem. Phys., 19, 28 360–28 380, 2017.

Jassoy, J. J., Berndhäuser, A., Duthie, F., Kühn, S. P., Hagelueken, G., and Schiemann, O.: Versatile trityl spin labels for nanometer distance measurements on biomolecules in vitro and within cells, Angew. Chem., 56, 177–181, 2017.

Jeschke, G.: DEER distance measurements on proteins, Ann. Rev. Phys. Chem., 63, 419–446, 2012.

Jeschke, G.: The contribution of modern EPR to structural biology, Emerg. Top. Life Sci., 2, 9–18, 2018.

Jeschke, G., Chechik, V., Ionita, P., Godt, A., Zimmermann, H., Banham, J., Timmel, C., Hilger, D., and Jung, H.: DeerAnalysis2006—a comprehensive software package for analyzing pulsed ELDOR data, Appl. Magn. Reson., 30, 473–498, 2006.

Jeschke, G., Sajid, M., Schulte, M., and Godt, A.: Three-spin correlations in double electron–electron resonance, Phys. Chem. Chem. Phys., 11, 6580–6591, 2009.

Jeschke, G., Sajid, M., Schulte, M., Ramezanian, N., Volkov, A., Zimmermann, H., and Godt, A.: Flexibility of shape–persistent molecular building blocks composed of p-phenylene and ethynylene units, J. Am. Chem. Soc., 132, 10 107–10 117, 2010.

Joseph, B., Tormyshev, V. M., Rogozhnikova, O. Y., Akhmetzyanov, D., Bagryanskaya, E. G., and Prisner, T. F.: Selective High-Resolution Detection of Membrane Protein–Ligand Interaction in Native Membranes Using Trityl–Nitroxide PELDOR, Angew. Chem., 55, 11 538–11 542, 2016.

Kaminker, I., Tkach, I., Manukovsky, N., Huber, T., Yagi, H., Otting, G., Bennati, M., and Goldfarb, D.: W-band orientation selective DEER measurements on a Gd3+/nitroxide mixed-labeled protein dimer with a dual mode cavity, J. Magn. Reson., 227, 66–71, 2013.

Kaminker, I., Bye, M., Mendelman, N., Gislason, K., Sigurdsson, S. T., and Goldfarb, D.: Distance measurements between manganese (II) and nitroxide spin-labels by DEER determine a binding site of Mn2+ in the HP92 loop of ribosomal RNA, Phys. Chem. Chem. Phys., 17, 15 098–15 102, 2015.

https://doi.org/10.5194/mr-2020-15
Preprint. Discussion started: 23 June 2020

Open Access MAGNETIC RESONANCE Discussions

Lueders, P., Jeschke, G., and Yulikov, M.: Double electron-electron resonance measured between Gd3+ ions and nitroxide radicals, J. Phys. Chem. Lett., 2, 604–609, 2011.

Lueders, P., Jäger, H., Hemminga, M. A., Jeschke, G., and Yulikov, M.: Distance measurements on orthogonally spin-labeled membrane spanning WALP23 polypeptides, J. Phys. Chem. B, 117, 2061–2068, 2013.

Martin, R. E., Pannier, M., Diederich, F., Gramlich, V., Hubrich, M., and Spiess, H. W.: Determination of end-to-end distances in a series of TEMPO diradicals of up to 2.8 nm length with a new four-pulse double electron electron resonance experiment, Angew. Chem., 37, 2833–2837, 1998.

Meyer, A. and Schiemann, O.: PELDOR and RIDME measurements on a high-spin manganese (II) bisnitroxide model complex, J. Phys. Chem. A, 120, 3463–3472, 2016.

Meyer, A., Abdullin, D., Schnakenburg, G., and Schiemann, O.: Single and double nitroxide labeled bis (terpyridine)-copper (II): Influence of orientation selectivity and multispin effects on PELDOR and RIDME, Phys. Chem. Chem. Phys., 18, 9262–9271, 2016.

Milov, A., Salikhov, K., and Shirov, M.: Use of the double resonance in electron spin echo method for the study of paramagnetic center spatial distribution in solids, Fizika Tverdogo Tela, 23, 975–982, 1981.

Milov, A., Ponomarev, A., and Tsvetkov, Y. D.: Electron-electron double resonance in electron spin echo: Model biradical systems and the sensitized photolysis of decalin, Chem. Phys. Lett., 110, 67–72, 1984.

Motion, C. L., Lovett, J. E., Bell, S., Cassidy, S. L., Cruickshank, P. A., Bolton, D. R., Hunter, R. I., El Mkami, H., Van Doorslaer, S., and Smith, G. M.: DEER sensitivity between iron centers and nitroxides in heme-containing proteins improves dramatically using broadband, high–field EPR, J. Phys. Chem. Lett., 7, 1411–1415, 2016.

Narr, E., Godt, A., and Jeschke, G.: Selective measurements of a nitroxide–nitroxide separation of 5 nm and a nitroxide–copper separation of 2.5 nm in a terpyridine-based copper (II) complex by pulse EPR spectroscopy, Angew. Chem., 41, 3907–3910, 2002.

Pannier, M., Veit, S., Godt, A., Jeschke, G., and Spiess, H. W.: Dead-time free measurement of dipole–dipole interactions between electron spins, J. Magn. Reson., 142, 331–340, 2000.

Plitzko, J. M., Schuler, B., and Selenko, P.: Structural biology outside the box—inside the cell, Curr. Opin. Struct. Biol., 46, 110–121, 2017.

Polyhach, Y., Bordignon, E., Tschaggelar, R., Gandra, S., Godt, A., and Jeschke, G.: High sensitivity and versatility of the DEER experiment on nitroxide radical pairs at Q-band frequencies, Phys. Chem. Chem. Phys., 14, 10 762–10 773, 2012.

Pribitzer, S., Sajid, M., Hülsmann, M., Godt, A., and Jeschke, G.: Pulsed triple electron resonance (TRIER) for dipolar correlation spectroscopy, J. Magn. Reson., 282, 119–128, 2017.

Qi, M., Hülsmann, M., and Godt, A.: Spacers for geometrically well–defined water–soluble molecular rulers and their application, J. Org. Chem., 81, 2549–2571, 2016a.

Qi, M., Hülsmann, M., and Godt, A.: Synthesis and Hydrolysis of 4–Chloro–PyMTA and 4–Iodo–PyMTA Esters and Their Oxidative Degradation with Cu(I/II) and Oxygen, Synthesis, 48, 3773–3784, 2016b.

Ritsch, I., Hintz, H., Jeschke, G., Godt, A., and Yulikov, M.: Improving the accuracy of Cu (ii)–nitroxide RIDME in the presence of orientation correlation in water-soluble Cu (ii)–nitroxide rulers, Phys. Chem. Chem. Phys., 21, 9810–9830, 2019.

Shevelev, G. Y., Krumkacheva, O. A., Lomzov, A. A., Kuzhelev, A. A., Trukhin, D. V., Rogozhnikova, O. Y., Tormyshev, V. M., Pyshnyi, D. V., Fedin, M. V., and Bagryanskaya, E. G.: Triarylmethyl labels: toward improving the accuracy of EPR nanoscale distance measurements in DNAs, J. Phys. Chem. B, 119, 13 641–13 648, 2015.

Spindler, P. E., Glaser, S. J., Skinner, T. E., and Prisner, T. F.: Broadband inversion PELDOR spectroscopy with partially adiabatic shaped pulses, Angew. Chem., 52, 3425–3429, 2013.

https://doi.org/10.5194/mr-2020-15
Preprint. Discussion started: 23 June 2020

Open Access MAGNETIC RESONANCE Discussions

Stoll, S. and Schweiger, A.: EasySpin, a comprehensive software package for spectral simulation and analysis in EPR, J. Magn. Reson., 178, 42–55, 2006.

Tait, C. E. and Stoll, S.: Coherent pump pulses in double electron electron resonance spectroscopy, Phys. Chem. Chem. Phys., 18, 18 470–18 485, 2016.

Teucher, M. and Bordignon, E.: Improved signal fidelity in 4-pulse DEER with Gaussian pulses, J. Magn. Reson., 296, 103–111, 2018.

Teucher, M., Zhang, H., Bader, V., Winklhofer, K. F., García-Sáez, A. J., Rajca, A., Bleicken, S., and Bordignon, E.: A new perspective on membrane-embedded Bax oligomers using DEER and bioresistant orthogonal spin labels, Sci. Rep., 9, 1–15, 2019.

Tschaggelar, R., Kasumaj, B., Santangelo, M. G., Forrer, J., Leger, P., Dube, H., Diederich, F., Harmer, J., Schuhmann, R., García-Rubio, I., et al.: Cryogenic 35GHz pulse ENDOR probehead accommodating large sample sizes: Performance and applications, J. Magn. Reson., 200, 81–87, 2009.

Valera, S., Ackermann, K., Pliotas, C., Huang, H., Naismith, J. H., and Bode, B. E.: Accurate extraction of nanometer distances in multimers by pulse EPR, Chem.: Eur. J., 22, 4700–4703, 2016.

von Hagens, T., Polyhach, Y., Sajid, M., Godt, A., and Jeschke, G.: Suppression of ghost distances in multiple-spin double electron–electron resonance, Phys. Chem. Chem. Phys., 15, 5854–5866, 2013.

Worswick, S. G., Spencer, J. A., Jeschke, G., and Kuprov, I.: Deep neural network processing of DEER data, Sci. Adv., 4, eaat5218, 2018.

Yulikov, M.: Spectroscopically orthogonal spin labels and distance measurements in biomolecules, EPR, 24, 1–31, 2015.